Optica Applicata, Vol. XXXVII, No. 1–2, 2007

Spectroscopic studies of Er-doped Si-rich silicon oxide/SiO_2 multilayers

FABRICE GOURBILLEAU*, CHRISTIAN DUFOUR, ROGER MADELON, RICHARD RIZK

SIFCOM, UMR CNRS 6176, ENSICAEN, 6 Bd Maréchal Juin, 14050 Caen Cedex

*Corresponding author: F. Gourbilleau, fabrice.gourbilleau@ensicaen.fr

The effects of Si nanocluster (Si-nc) size and of the distance between Si-nc and Er ion on the photoluminescence of the Er^{3+} ions have been investigated by means of appropriate multilayer configurations fabricated by reactive magnetron sputtering. On the one hand, the effect of Si-nc size is studied in Er-Si-rich SiO_2/SiO_2 multilayers. The coupling between Si-nc and Er^{3+} ions is found to be less efficient when the Si-nc's reach a size of 5 nm and attributed to a loss of the quantum confinement of carriers. On the other hand, the interaction distance between Si-nc and Er ions is determined through the photoluminescence properties of Si-rich SiO_2/Er-SiO_2 multilayers. The characteristic interaction distance Si-nc-Er is dependent on the nature of the sensitizers with 0.4 ± 0.1 nm for amorphous Si and 2.6 ± 0.4 nm for Si nanocrystals.

Keywords: reactive magnetron sputtering, multimayers, erbium, Si nanoclusters, photoluminescence, interaction distance.

1. Introduction

The development of miniaturized optoelectronic devices or photonic components during these last years has led the scientific community to study new systems offering suitable properties or promising potentiality in such field. One of the most promising systems is the Si-based one due to its compatibility with the Si technology. In this context, besides the interesting photoluminescence properties of Si nanostructures [1–6], Er-doped Si-SiO_2 materials in composite or multilayered structures attract the huge interest because it gives strong luminescence at 1.54 μm which is standard wavelength used in telecommunication.

In fact, in such a system, the luminescence intensity of Er^{3+} ions is 100 times higher in comparison to the one obtained from such ion in pure SiO_2. This behaviour is linked to the quantum confinement of the carriers when the Si nanocrystals reach the nanometer scale. The pumping laser excites the Si nanocrystals which will then transfer efficiently their energy to the neighbouring Er^{3+} ions [7–11]. The consequence of such physical phenomena is an effective absorption cross section σ_{abs}^{Eff} of Er comparable

to that of Si-nc, *i.e.*, 10^{-16} cm^{-2} whereas σ_{abs} of Er in pure SiO_2 matrix is about 10^{-20} cm^{-2} [12–14]. Such properties pave the way to the fabrication of miniaturized Er-doped Si-SiO_2 amplifying systems.

However, the optimization of the coupling rate between Si-nanocluster (Si-nc) and Er^{3+} ion is needed to fabricate the more efficient device. This can be achieved through the determination of some specific parameters governing the energy transfer between these two entities. One of them is the critical size of the Si-nc above which the Er photoluminescence intensity strongly decreases. FRANZÒ *et al.* [15] reported that few atoms of Si (~50) are sufficient to play their role of sensitizer towards Er ions and more recently, TIMOSHENKO *et al.* [16] have studied, in a much lesser extent, the effect of Si-nc size on the luminescence emission at 1.54 μm. Anyway, no information is provided on the size upper limit of these nanoclusters above which no energy transfer can occur. The critical distance separating Si-nc and Er^{3+} ions is also one of these main parameters. Recently, KIMURA *et al.*[17] have reported a characteristic interaction distance of 2–3 nm for Er-doped system containing crystallized Si-nc while JHE *et al*. [18] found 0.5 ± 0.1 nm for amorphous Si/Er-SiO_2 multilayers. In this paper we propose to develop the studies leading to the determination of these relevant parameters, *i.e.*, the critical interaction distance between Er ions and Si-nc and the optimum Si-nc size on the efficiency of the energy transfer to the rare earth ion. The layers considered hereafter have been deposited by reactive magnetron sputtering and consist in a stacking of silicon-rich silicon oxide (SRSO)/SiO_2 doped with Er in either SRSO or SiO_2 layers of various thicknesses.

2. Experimental

The process developed to fabricate the multilayer (ML) structure consists in the alternative magnetron sputtering of a pure SiO_2 target in the mixture of Ar and H_2 or in pure Ar atmosphere to deposit silicon rich silicon oxide (SRSO) or silicon oxide layers, respectively. The hydrogen ratio r_H, *i.e.*, the ratio of hydrogen to the total gas flow rate $r_H = P_{H_2}/P_{tot}$ was kept at 50% and the substrate deposition temperature was 650 °C. As a source of silicon a pure SiO_2 target was used, hydrogen reduces the oxygen concentration in plasma what in consequence allows to incorporate a Si excess in the deposited layer (SRSO). The Er has been incorporated either in SRSO or in SiO_2 sublayers according the following procedure:

– Er-SRSO/SiO_2 multilayers called ML_1 (see hereafter Fig. 3) were fabricated by sputtering a silica target topped with Er_2O_3 pellets using a mixture of H_2 and Ar or a bare SiO_2 target (free of Er_2O_3 pellets) under pure argon plasma;

– SRSO/Er-SiO_2 multilayers called ML_2 (see hereafter Fig. 3) were obtained using the same procedure but by changing the plasma gas upon the silica target topped with Er_2O_3 pellets (plasma with Ar) and a bare SiO_2 target free of Er_2O_3 pellets (plasma with r_H = 50%).

The multilayers were subsequently annealed at 900 °C under a flux of N_2 containing 5% of H_2. The cross-sectional microstructure of the deposited samples has

been investigated by using high resolution electron microscope (HREM) type TOPCON EM 002B operating at 200 keV. The photoluminescence emission spectra have been recorded at room or liquid He temperatures under resonant (488 nm) and non resonant (476.5 nm) lines of an Ar^+ laser. The emitted signal was recorded by using a 1 m single monochromator equipped with liquid nitrogen cooled Ge detector. For the photoluminescence lifetime, the laser beam was chopped at a frequency of 15 Hz and its power density was reduced to about 3 $mW.cm^{-2}$. The overall time response of the experimental setup is about 0.5 ms.

3. Results and discussion

The HREM micrographs collected in Fig. 1 show the microstructure of the annealed multilayers for three different SRSO sublayer thickness values (t_{SRSO}), *i.e.*, 1.8 nm, 3.8 nm and 5 nm. As one can observe for t_{SRSO} = 1.8 nm, no Si-nc have been formed even after an annealing treatment, whereas for higher t_{SRSO}, the Si-nc are clearly visible and their size corresponds to the sublayer thickness. The absence of any crystallization for t_{SRSO} = 1.8 nm has been previously noticed for similar multilayered structures [19] and has been attributed to the high interface/layer ratio that requires higher annealing temperature than the 900 °C used here for favouring the crystallization of the Si nanocrystallites [20].

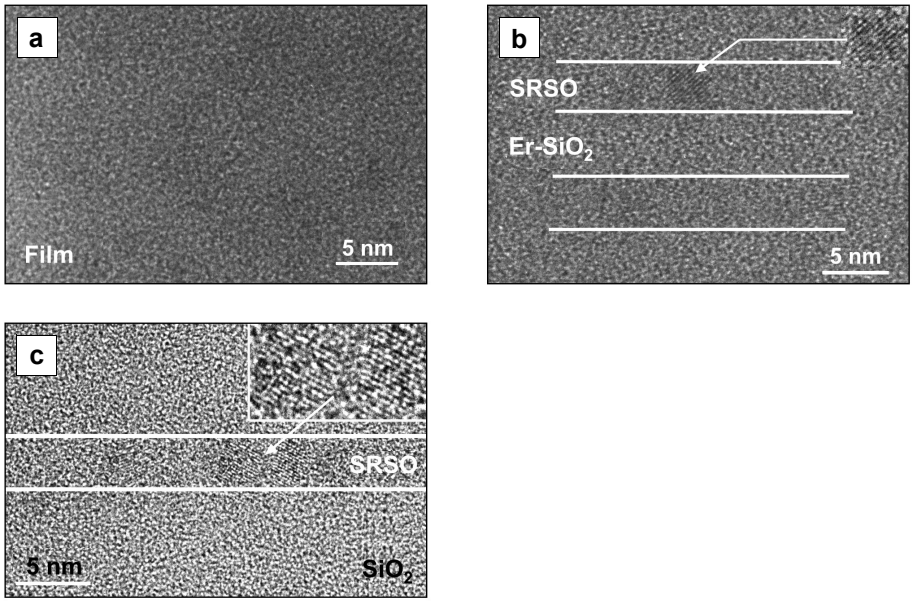

Fig. 1. Typical HREM images of the multilayers for different Si-rich silicon oxide sublayer thicknesses (t_{SRSO}) sandwiched between two SiO_2 sublayers : t_{SRSO} = 1.8 nm (**a**), t_{SRSO} = 3.8 nm (**b**), t_{SRSO} = 5 nm (**c**). Some Si nanocrystals can be seen in (**b**) and (**c**) and their insets show a magnified image of the nanocrystal.

Figure 2 displays the comparison between photoluminescence spectra of Er-doped SiO_2 layer free from any Si excess and an Er-SRSO/SiO_2 multilayer with t_{SRSO} = 1.8 nm under a non resonant excitation line (476.5 nm). Concerning the sample containing no Si excess, no photoluminescence (PL) signal can be detected whereas in the case of the ML_1 film, an intense PL emission at 1.54 μm is observed which indicates the role of Si-nc acting as sensitizers to transfer efficiently their energy to the neighbouring Er^{3+} ions. Moreover, the resulting PL emission from these

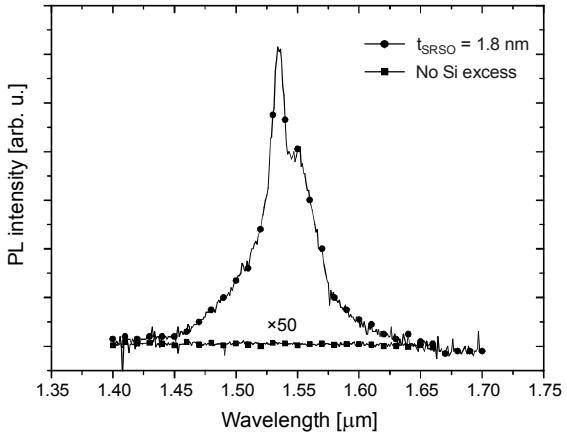

Fig. 2. PL spectra of a Er-doped SiO_2 layer containing no Si excess and a Er-SRSO/SiO_2 multilayer.

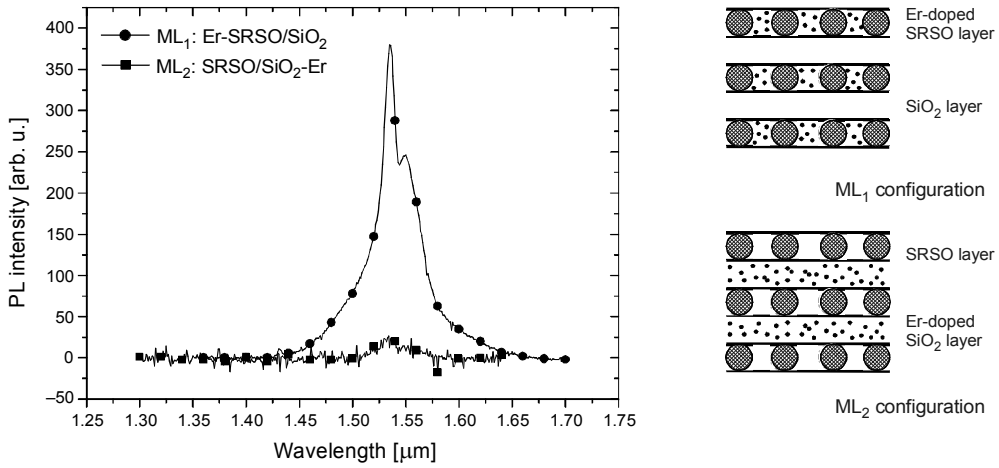

Fig. 3. Comparison of the PL spectra obtained from a Er-SRSO/SiO_2 and a SRSO/Er-SiO_2 multilayers. The schematic drawing of the two configurations of the multilayers, ML_1 and ML_2 is displayed on the right part of the figure.

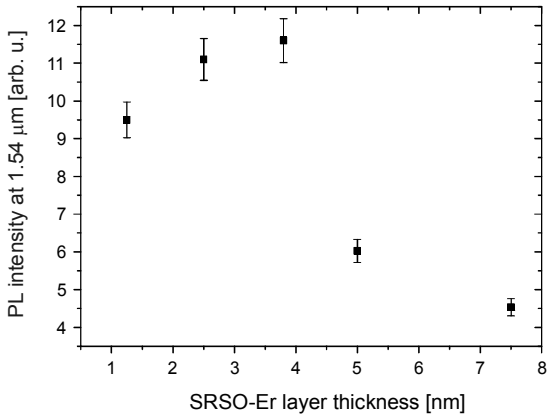

Fig. 4. Evolution of the Er^{3+} emission at 1.54 μm for the Er-SRSO/SiO_2 multilayers as a function of the Er-SRSO sublayer thickness.

multilayers for which all Si nanograins are amorphous as described above, demonstrates that the presence of Si nanocrystallites is not a prerequisite for an efficient energy transfer process towards the Er^{3+} ions. This is in agreement with previous results obtained for Er-doped composite layers obtained by different fabrication deposition methods [21, 22].

The Figure 3 shows PL spectra excited with the non resonant 476.5 nm line for the samples having ML_1 and ML_2 configuration. The schematic representation of the multilayers is added on the right of the figure. Both configurations contain the same Er amount. The emission of the ML_1 configuration is about ten times higher than that of the ML_2 one. The above results show that the location of the Er ions plays an essential role in excitation and energy transfer process between Er and sensitizers.

The effect of the sensitizer size on the efficiency of the Si-nc-Er coupling rate is now studied through the PL emission from the ML_1 type structure with different SRSO sublayer thicknesses varied from 1 to 7.5 nm, *i.e.*, the size of the Si-nc nanograins between then same values (Fig. 4). It appears that, under the non resonant Ar^+ line excitation, the PL emission first increases with t_{SRSO} increase and then abruptly decreases when this thickness reaches the value of 5 nm. Such behaviour can attributed to:

– either to the formation of larger Si nanoclusters which are less efficient in energy transfer towards the Er^{3+} ions due to the loss of the quantum confinement of carriers when the size becomes comparable to the Bohr radius of the generated exciton (5 nm);

– or to an energy back transfer process which appears when the erbium level is resonant with that of Si [23–25]. Such process can occur for large Si grains (≥ 5 nm) due to the shrinkage of the nanograin bandgap towards that of bulk Si.

T a b l e. Ratio of the PL intensity and emission lifetime at 1.54 μm measured at 10 and 300 K, $I_{(10K)}/I_{(300K)}$ and $\tau_{(10K)}/\tau_{(300K)}$, respectively, for different thicknesses of the Er-doped SRSO sublayer in the ML_1 configuration. For comparison, the corresponding values obtained on bulk Si crystal (see [16, 17]) are reported.

Sample	$I_{(10K)}/I_{(300K)}$	$\tau_{(10K)}/\tau_{(300K)}$
Bulk Si (monocrystalline)	1000 (refs. [16, 17])	140 (ref. [16])
t_{SRSO} = 1.8 nm	2.5	1.1
t_{SRSO} = 3.8 nm	2.3	1.3
t_{SRSO} = 5.0 nm	1.0	1.2

To settle between these two probable origins, the influence of the temperature on the PL intensity and Er PL lifetime has been studied. The PL measurements have been done between 10 K and 300 K for the ML_1 structures having different values of t_{SRSO}. The results for the two extreme temperatures (10 and 300 K) are summarized in the Table and compared with values reported in the literature for bulk Si implanted by Er [24, 25]. The ratio of $I_{(10K)}/I_{(300K)}$ is considerably different than that found for Er-bulk Si and indicate on the absence of PL temperature quenching. This is supported by the ratio of $\tau_{(10K)}/\tau_{(300K)}$ which is also considerably different than that obtained for Er-bulk Si. The dependence of I_{PL} at 1.54 μm on Si-nc size indicate on the loss of quantum confinement of carriers leading to a loss of the efficiency in the energy transfer to the Er^{3+} ions when Si-nc reaches the size of 5 nm . The fact that the PL has not totally vanished is an indication of the presence of Si nanograins smaller than 5 nm, probably amorphous as they have not been seen by HREM, but which ensure the Er excitation.

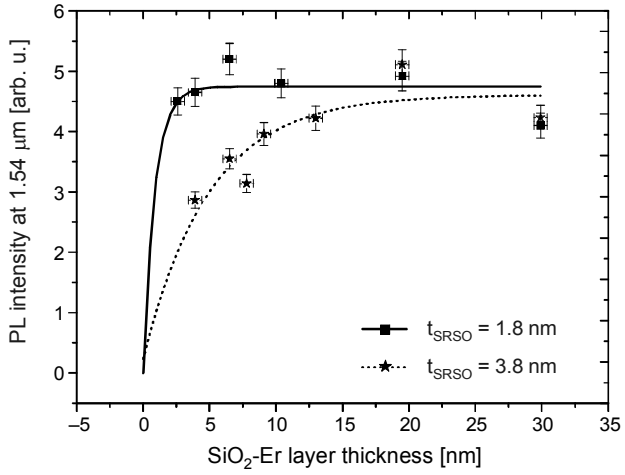

Fig. 5. Evolution of the Er^{3+} emission at 1.54 μm with the thickness of the Er-doped SiO_2 sublayer thickness for two t_{SRSO}, 1.8 nm and 3.8 nm. The lines are the results of the simulation based on the exchange interaction mechanism decreasing as an exponential law ($\exp(x/x_0)$).

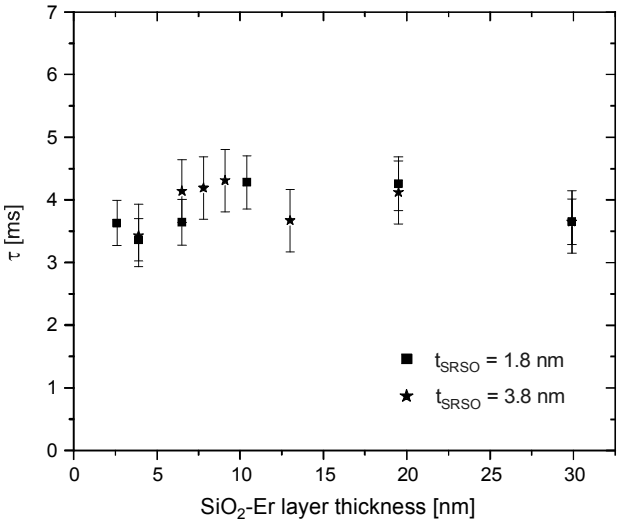

Fig. 6. Er^{3+} photoluminescence lifetime for different SiO_2-Er sublayer thicknesses and two t_{SRSO} in the case of the ML_2 configuration.

Let us examine now the evolution of the PL intensity at 1.54 μm when the thickness of the Er-doped SiO_2 sublayer increases in the ML_2 configuration. One can expect first a raise of the PL intensity with increase of the number of Er^{3+} excited through the Si nanograins present on both sides of the SiO_2-Er sublayer. The increase of the SiO_2-Er sublayer thickness leads to the saturation of the recorded PL signal because the Er^{3+} ions located far from Si-nc will not be excited.

Figure 5 reports the I_{PL} data at 1.54 μm as a function of SiO_2-Er sublayer thickness for two values of t_{SRSO} providing either amorphous (t_{SRSO} = 1.8 nm) or crystallized (t_{SRSO} = 3.8 nm) Si nanograins. Both dependences show similar behaviour with the expected evolution of the Er^{3+} PL emission. One can note that the saturation regime is reached earlier for the thinnest t_{SRSO} value. Figure 6 shows the dependence of the Er^{3+} photoluminescence lifetimes on the SiO_2-Er sublayer thickness for both values of t_{SRSO}. The absence of any dependence on the SiO_2-Er sublayer thickness attests of the equal quality of the materials and confirms that the evolution of I_{PL} described above is only dependent on the number of the excited Er^{3+} ions. In such experiments, *i.e.*, steady state and weak pumping regime, one can consider that the number of excited Er^{3+} ions, N_{Er}^{*} at a distance x from the sensitizer (Si-nc) can be approximated to:

$$N_{Er}^{*} \cong F(x)\,\tau N_{Er}^{0} \quad \text{if} \quad F(x)\tau \ll 1$$

where N_{Er}^{0} is the number of total excitable Er^{3+}, τ – the PL lifetime and $F(x)$ – the distance dependent excitation rate [18]. The function $F(x)$ is a decreasing function which describes the interaction between Si-nc and Er^{3+}. Two functions are usually

used for describing such a mechanism: a resonant dipole–dipole interaction decreasing as x^{-6} and an exchange interaction following an exponential law $\exp(x/x_0)$ [26, 27]. The data of the Fig. 5 have been fitted with the both laws (power and exponential) and the best results have been obtained considering an exchange interaction process (*i.e.*, $\exp(x/x_0)$). The deduced interaction distances are $x_0 = 0.8$ nm for $t_{SRSO} = 1.8$ nm and $x_0 = 5.2$ nm for $t_{SRSO} = 3.8$ nm with an uncertainty of 20%. However, in such configuration, the recorded I_{PL} results from the excitation of Er^{3+} from two adjacent SRSO sublayers. Consequently, the determined x_0 value is the double of the characteristic interaction distance. We found thus $x_0 = 0.4 \pm 0.1$ nm for $t_{SRSO} = 1.8$ nm and $x_0 = 2.6 \pm 0.4$ nm for $t_{SRSO} = 3.8$ nm. If we compare these values with that recently provided by the literature, one can notice that:

– the lowest x_0 value is close to the 0.5 ± 0.1 nm reported by JHE *et al.* [18] in the case of amorphous Si/SiO_2 multilayers;

– the highest x_0 value is in the 2–3 nm range proposed by KIMURA *et al.* [17] in the case of crystalline porous Si doped with Er.

Thus our results obtained on the same materials fabricated using the same process have confirmed and demonstrated that x_0 can reach two values depending on the structure of the sensitizers (amorphous or crystalline). JHE *et al.* [18] have proposed a possible influence of the Si phase on the carrier-Er interaction. Thus, one possible explanation of the existence of two x_0 values can be linked to the carrier wavefunction localization. In this connection, the carrier wavefunctions for $t_{SRSO} = 1.8$ nm would be localized at the interface and the interaction distance between Si nanograins and Er is defined by the distance from the interface Si/SiO_2 to the Er^{3+} ion. The larger x_0 value obtained for $t_{SRSO} = 3.8$ nm can be explained by carrier wavefunctions extended within the nanocrystals which require to take into account the nanocrystal radius dependence of x_0.

4. Conclusions

This work provides more insight of the Si-nc coupling rate by determining two relevant spectroscopic parameters: the optimum value of Si-nc size and the characteristic interaction distance between Si nanograin and Er^{3+} ions. The effect of Si-nc size on the Er^{3+} emission is examined in Er-doped $SRSO/SiO_2$ multilayers. It appeared that the Si nanograins play their role of efficient sensitizers towards Er^{3+} ions since its size is lower than 5 nm. For higher size, the decrease of the Er^{3+} PL emission is attributed to the loss of the quantum confinement of carriers. The evolution of the PL intensity at 1.54 μm as a function of the distance Si-Er (x) for the $SRSO/SiO_2$-Er multilayers, follows an exponential decrease, $\exp(x/x_0)$, which corresponds to an exchange Er-carrier interaction. The characteristic interaction distance is found to be dependent on the nature of the Si phase. In presence of amorphous SRSO sublayer, x_0 is equal to 0.4 ± 0.1 nm whereas for Si nanocrystals, this distance is about 2.6 ± 0.4 nm. These results seem to evidence the necessity to account for the nanocrystal radius dependence of x_0. Further investigations are in progress to confirm this tendency.

References

[1] CANHAM L.T., *Silicon quantum wire array fabrication by electrochemical and chemical dissolution of wafers*, Applied Physics Letters **57**(10), 1990, pp. 1046–8.

[2] SHIMIZU-IWAYAMA T., FUJITA F., NAKAO S., SAITOH S., FUJITA T., ITOH N., *Visible photoluminescence in Si^+-implanted silica glass*, Journal of Applied Physics **75**(12), 1994, pp. 7779–83.

[3] CHARVET S., MADELON R., GOURBILLEAU F., R. RIZK, *Spectroscopic ellipsometry analyses of sputtered Si/SiO_2 nanostructures*, Journal of Applied Physics **85**(8), 1999, pp. 4032–9.

[4] FERNANDEZ B.G., LÓPEZ M., GARCÍA C., PÉREZ-RODRÍGUEZ A., MORANTE J.R., BONAFOS C., CARRADA M., CLAVERIE A., *Influence of average size and interface passivation on the spectral emission of Si nanocrystals embedded in SiO_2*, Journal of Applied Physics **91**(2), 2002, pp. 798–807.

[5] GOURBILLEAU F., PORTIER X., TERNON C., VOIVENEL P., MADELON R., RIZK R., *Si-rich/SiO_2 nanostructured multilayers by reactive magnetron sputtering*, Applied Physics Letters **78**(20), 2001, pp. 3058–60.

[6] ZACHARIAS M., HEITMANN J., SCHOLZ R., KAHLER U., SCHMIDT M., BLÄSING J., *Size-controlled highly luminescent silicon nanocrystals: a SiO/SiO_2 superlattice approach*, Applied Physics Letters **80**(4), 2002, pp. 661–3.

[7] FUJII M., YOSHIDA M., KANZAWA Y., HAYASHI S., YAMAMOTO K., *1.54 μm photoluminescence of Er^{3+} doped into SiO_2 films containing Si nanocrystals: Evidence for energy transfer from Si nanocrystals to Er^{3+}*, Applied Physics Letters **71**(9), 1997, pp. 1198–200.

[8] SHIN J.H., KIM M., SEO S., LEE C., *Composition dependence of room temperature 1.54 μm Er^{3+} luminescence from erbium-doped silicon:oxygen thin films deposited by electron cyclotron resonance plasma enhanced chemical vapor deposition*, Applied Physics Letters **72**(9), 1998, pp. 1092–4.

[9] CHRYSSOU C.E., KENYON A.J., IWAYAMA T.S., PITT C.W., HOLE D.H., *Evidence of energy coupling between Si nanocrystals and Er^{3+} in ion-implanted silica thin films*, Applied Physics Letters **75**(14), 1999, pp. 2011–3.

[10] FRANZÒ G., PACIFICI D., VINCIGUERRA V., PRIOLO F., IACONA F., IACONA F., *Er^{3+} ions–Si nanocrystals interactions and their effects on the luminescence properties*, Applied Physics Letters **76**(16), 2000, pp. 2167–9.

[11] KIK P., BRONGERSMA M.L., POLMAN A., *Strong exciton-erbium coupling in Si nanocrystal-doped SiO_2*, Applied Physics Letters **76**(17), 2000, pp. 2325–7.

[12] FUJII M., YOSHIDA M., HAYASHI S., YAMAMOTO K., *Photoluminescence from SiO_2 films containing Si nanocrystals and Er: Effects of nanocrystalline size on the photoluminescence efficiency of Er^{3+}*, Journal of Applied Physics **84**(8), 1998, pp. 4525–31.

[13] PRIOLO F., FRANZÒ G., PACIFICI D., VINCIGUERRA V., IACONA F., IRRERA A., *Role of the energy transfer in the optical properties of undoped and Er-doped interacting Si nanocrystals*, Journal of Applied Physics **89**(1), 2001, pp. 264–72.

[14] KENYON A.J., CHRYSSOU C.E., PITT C.W., SHIMIZU-IWAYAMA T., HOLE D.E., SHARMA N., HUMPHREYS C.J., *Luminescence from erbium-doped silicon nanocrystals in silica: Excitation mechanisms*, Journal of Applied Physics **91**(1), 2002, pp. 367–74.

[15] FRANZÒ G., BONINELLI S., PACIFICI D., PRIOLO F., IACONA F., BONGIORNO C., *Sensitizing properties of amorphous Si clusters on the 1.54 μm luminescence of Er in Si-rich SiO_2*, Applied Physics Letters **82**(22), 2003, pp. 3871–3.

[16] TIMOSHENKO YU.V., LISACHENKO M.G., KAMENEV B.V., SHALYGINA O.A., KASHKAROV P.K., HEITMANN J., SCHMIDT M., ZACHARIAS M., *Highly efficient sensitizing of erbium ion luminescence in size-controlled nanocrystalline Si/SiO_2 superlattice structures*, Applied Physics Letters **84**(14), 2004, pp. 2512–4.

[17] KIMURA T., ISSHIKI H., IDE S., SHIMIZU T., ISHIDA T., SAITO R., *Suppression of Auger deexcitation and temperature quenching of the Er-related 1.54 μm emission with an ultrathin oxide interlayer in an Er/SiO_2/Si structure*, Journal of Applied Physics **93**(5), 2003, pp. 2595–601.

[18] JHE J.H., SHIN J.H., KIM K.J., MOON D.W., *The characteristic carrier-Er interaction distance in Er-doped a-Si/SiO_2 superlattices formed by ion sputtering,* Applied Physics Letters **82**(25), 2003, pp. 4489–91.

[19] TERNON C., DUFOUR C., GOURBILLEAU F., RIZK R., *Roles of interfaces in nanostructured silicon luminescence*, European Physical Journal B **41**(3), 2004, pp. 325–32.

[20] LOCKWOOD D.J., GROM G.F., TSYBESKOV L., FAUCHET P.M., LABBÉ H.J., MCCAFFREY J.P., WHITE B., *Self-organization and ordering in nanocrystalline Si/SiO_2 superlattices*, Physica E: Low-Dimensional Systems and Nanostructures **11**(2–3), 2001, pp. 99–103.

[21] RAN G.Z., CHEN Y., YUAN F.C., QIAO Y.P., FU J.S., MA Z.C., ZONG W.H., QIN G.G., *An effect of Si nanoparticles on enhancing Er^{3+} electroluminescence in Si-rich SiO_2:Er films*, Solid State Communications **118**(11), 2001, pp. 599–602.

[22] GOURBILLEAU F., LEVALOIS M., DUFOUR C., VICENS J., RIZK R., *Optimized conditions for an enhanced coupling rate between Er ions and Si nanoclusters for an improved 1.54 μm emission*, Journal of Applied Physics **95**(7), 2004, pp. 3717–22.

[23] MICHEL J., BENTON J.L., FERRANTE R.F., JACOBSON D.C., EAGLESHAM D.G., FITZGERALD E.A., XIE Y.-H., POATE J.M., KIMERLING L.C., *Impurity enhancement of the 1.54 μm Er^{3+} luminescence in silicon*, Journal of Applied Physics **70**(5), 1991, pp. 2672–8.

[24] KIK P.G., DE DOOD M.J.A., KIKOIN K., POLMAN A., *Excitation and deexcitation of Er^{3+} in crystalline silicon*, Applied Physics Letters **70**(13), 1997, pp. 1721–3.

[25] PRIOLO F., FRANZÒ G., COFFA S., CARNERA A., *Excitation and nonradiative deexcitation processes of Er^{3+} in crystalline Si*, Physical Review B **57**(8), 1998, pp. 4443–55.

[26] SUCHOCKI A., LANGER J.M., *Auger effect in the Mn^{2+} luminescence of CdF_2:(Mn,Y) crystals*, Physical Review B **39**(11), 1989, pp. 7905–16.

[27] SNOEKS E., KIK P.G., POLMAN A., *Concentration quenching in erbium implanted alkali silicate glasses*, Optical Materials **5**(3), 1996, pp. 159–67.

Received December 15, 2005
in revised form March 27, 2007